

CHARACTERISTICS OF STRONG GROUND MOTION  
- ACCELERATION RECORDS IN NORTHERN PART OF JAPAN -

Tomoyuki Inukai (I)  
Hidehiko Miyahara (II)  
Takao Nishikawa (III)  
Presenting Author: T. Inukai

SUMMARY

This paper presents an analysis of characteristics of strong ground motions obtained at seven observation stations located in northern part of Japan. The shapes of the Fourier spectrum, the relationships between the peak frequency and the magnitude, and also maximum acceleration, maximum velocity, and spectrum intensity were discussed for each station respectively. The Fourier spectrum of each station were classified into three types of pattern according to the surface soil conditions. The relation between each parameter had a good correlation to the predominant period of strong ground motions.

INTRODUCTION

It is known that Japanese earthquake motion may be very much effected by the surface soil conditions. It is necessary to make it clear the relationship between the characteristics of earthquake ground motions and the conditions of the surface soil to bedrock for earthquake proof design (Ref. 1). If the common characteristics could be found in the various ground motion records observed in one place, the characteristics of soil conditions could be determined and also its characteristics would be available for earthquake proof design of structures. Totally more than 120 ground motion records observed in northern part of Japan, there were seven observation stations, were analysed by Fourier analyses and also response analyses. For each station the characteristics of strong ground motions, predominant frequency, maximum acceleration, maximum velocity, and spectrum intensity, were discussed.

ACCELERATION RECORDS OF STRONG GROUND MOTIONS

Acceleration records of strong ground motions based on Technical Note of the Port and Harbor Research Institute were obtained at seven observation stations located in northern part of Japan along the coast of the Pacific Ocean; Kushiro (HK004), Muroran (HK003), Aomori (TH020), Hachinohe (TH029), Miyako (TH014), Shiogama (TH033), and Ofunato (TH019). These acceleration records were obtained by the SMAC-B2 accelerographs ( Natural period is 0.14 second, damping is critical, and damping mechanism is air piston. ) installed on the simple shallow foundations. From 1965 to 1980,

- 
- (I) Research staff of Takenaka Technical Research Laboratory, Tokyo, Japan
  - (II) Construction engineer of Kajima Construction Co., Ltd., Tokyo, Japan
  - (III) Associate Professor of Tokyo Metropolitan University, Tokyo, Japan

frequencies read from the Power spectrum for Aomori (TH020), Miyako (TH014), Hachinohe (TH029), and Shiogama (TH033) were shown in Figs. 7. In these figures ● and ▲ indicate the predominant frequencies where the amplitude of spectrum had a maximum, and ○ and △ indicate the other predominant frequencies. Also the predominant frequencies obtained from the long-period range microtremores observations after the 1968 Tokachi-Oki Earthquake (Ref. 3) were shown in Figs. 7 by broken lines. It was shown that the frequencies which had a maximum amplitude of spectrum became lower as the magnitude increased. But this tendency was not recognized clearly in Fig. 7-b where the high frequency range of the spectrum (about 5 Hz) was predominated because of the shallow surface layer conditions. It was shown that the lower limit of the frequencies which had a maximum amplitude of the spectrum in each station (0.3 Hz at Aomori, 0.4 Hz at Hachinohe, and 5.0 Hz at Miyako) sufficiently corresponded to the results of the microtremores observations.

#### PREDOMINANT PERIOD AND ANOTHER CHARACTERISTICS

The relationships between the predominant period of the ground motion accelerations  $T_g$  where the Power spectrum had a maximum amplitude and maximum acceleration  $A_m$ , maximum velocity  $V_m$ , and spectrum intensity  $SI$ , which would very much concern with the ground motion intensity, were investigated for all records. The spectrum intensity defined by Housner was as follows (Ref. 4);

$$SI = \int_{0.1}^{2.5} Sv(T,h) dT \quad \dots\dots\dots (2)$$

where,  $Sv(T,h)$  was the velocity response spectrum value corresponding to the period  $T$  and damping  $h$  of structure. In this analysis,  $h$  and  $dT$  were taken as 20% and 0.05 second respectively.

In Fig. 8, the relationship between the ratio of the maximum acceleration to the maximum velocity,  $A_m/V_m$ , and the predominant period  $T_g$  was shown. There was a good correlation in the both parameters. The relationship between the maximum acceleration to the spectrum intensity,  $A_m/SI$ , and the predominant period was shown in Fig. 9, where existed a good correlation, too. Fig. 10 was shown that the ratio of the maximum velocity to the spectrum intensity,  $V_m/SI$ , did not change with the predominant period. The relationship between the product of  $A_m/V_m$  and  $T_g$  and the predominant period was shown in Fig. 11, where did not exist the constant relation (Ref. 5) and existed a good positive correlation. The relations between each parameter determined by least-squares approximation method were as follows;

$$\log(A_m/V_m) = -0.513 \log(T_g) + 0.91 \quad \dots\dots\dots (3)$$

$$\log(A_m/SI) = -0.606 \log(T_g) + 0.47 \quad \dots\dots\dots (4)$$

$$\log(V_m/SI) = -0.092 \log(T_g) - 0.44 \quad \dots\dots\dots (5)$$

$$\log(A_m \cdot T_g / V_m) = 0.487 \log(T_g) + 0.91 \quad \dots\dots\dots (6)$$

From these relationships, assuming that the maximum accelerations of the ground motions had the same value in each stations, the ground motions recorded at the observation station, which had the long predominant period soil conditions, should have larger maximum velocity and spectrum intensity compared to those values obtained from the ground motions recorded at the observation station which had the short predominant period soil conditions.

totally more than 120 accelerations of strong ground motions with almost maximum accelerations exceeding 20 gals have been obtained including the 1968 Tokachi-Oki Earthquake records, the 1978 Miyagi-Ken-Oki Earthquake records which gave severe damage to many structures. The location of the observation stations and of the epicenters were shown in Fig. 1. The numbers attached to the stations and the epicenters in Fig. 1 were based on Strong-Motion Earthquake Records in Japan (Ref. 2). For example, 199, 200, and 202 shows the epicenter of the 1968 Tokachi-Oki Earthquake and its aftershocks respectively, and 789 shows the 1978 Miyagi-Ken-Oki Earthquake. The number of the strong ground motions classified into several groups according to the value of maximum accelerations were shown in Fig. 2. And the number of the magnitude classified into several level were shown in Fig. 3. The magnitude was determined by Tsuboi's formula:

$$M = \log(A) + 1.73\log(E) - 0.83 \quad \dots\dots\dots (1)$$

where M was the magnitude, A was the maximum amplitude in micron, and E was the epicentral distance in km. The relations between magnitude and epicentral distance in each station were shown in Figs. 4.

#### ACCELERATION RECORDS PROCESSING

To investigate the frequency characteristics of the acceleration records shorter than 10 Hz, the instruction correction of SMAC-B2 was not applied to these records in frequency domain. In calculating the velocity from the acceleration record, so as to neglect the effects of long-period components of the acceleration record, it was used the low-cut filter which was attenuating in the shape of cosine-curve from 0.2 Hz to 0.1 Hz. And its inverse Fourier transforms, low-cut acceleration record in time domain, was numerically integrated by trapezoidal rule. The relationships between maximum acceleration and maximum velocity for each station were shown in Figs. 5. In Fourier analyses, the sampling time was taken as 0.01 second, and Fast Fourier Transform (FFT) was used. The Fourier and Power spectrum were smoothed by Parzen spectral window.

#### PREDOMINANT FREQUENCIES OF ACCELERATION RECORDS

To investigate the frequency characteristics of the acceleration records effected the surface soil conditions, the Fourier spectrum in each station ( normalized the value of the maximum acceleration to 1 gal and smoothed by Parzen window with band width 0.4 Hz ) were shown in Figs. 6. Each spectrum of ground motion in each observation station indicated similar form. The difference of the predominant frequencies determined from the Fourier spectrum of each station with different surface soil conditions was understood. These spectrum were classified into three types of pattern according to the surface soil conditions. The first one was the spectrum which had a peak in low frequency range; Ofunato (THO19), Aomori (THO20), and the second one was the spectrum which had a peak in fairly high frequency range; Miyako (THO14), and the third one was the spectrum which had plural peaks; Kushiro (HK004).

Further to understand above mentioned relationships quantitatively, the relationships between the magnitude of each earthquake and the peak

Because of the good correlations between the predominant period and the other parameters of the strong ground motions,  $A_m/V_m$ ,  $A_m/SI$ ,  $V_m/SI$ , and  $A_m \cdot T_g/V_m$ , if the predominant period would be decided in one place, the other parameters could be estimated easily, and these results would be available for earthquake proof design of structures.

#### CONCLUDING REMARKS

1. The difference of the Fourier spectrum shapes of each observation station with the different surface soil conditions was understood. The shapes of the spectrum were classified into three types of pattern according to the surface soil conditions.
2. The predominant frequencies which had a maximum amplitude of the Fourier spectrum became lower as the magnitude increased. The lower limit of the predominant frequencies in each observation station corresponded to the results of the microtremores observations sufficiently.
3. Since there were the good correlations between the predominant period of the ground motion accelerations and the other parameters of the strong ground motion characteristics, if the predominant periods would be decided in one place, the value of the other parameters could be estimated easily. And the results would be available for earthquake proof design of structures.

#### ACKNOWLEDMENTS

The authors would like to express their appreciations to Mr. M. Sawada and Mr. T. Miyaoka for their works on these analyses, and Prof. Y. Osawa of the the Earthquake Research Institute Univ. of Tokyo and the staff of his laboratory for their guidance and encouragement through out this work, and the Earthquake Resistant Structures Laboratory of the Port and Harbor Research Institute for acceleration records used in these analyses.

#### REFERENCES

1. Kobayashi, H. and S. Nagahashi, "Amplification Characteristics of the Ground and Spectral Characteristics of Earthquake Motions on the Seismic Bedrock Inferred from Spectral Characteristics of Earthquake Motions Observed on the Ground Surface", Trans. of AIJ, No240, 1976, p79-92.
2. "Strong-Motion Earthquake Records in Japan", the National Research Center for Disaster Prevention Science and Technology Agency.
3. Kudo, K., Y. Ohta, and H. Kagami et al., "Observation of 1- to 5-sec Microtremores and their Application to Earthquake Engineering. Part III", Zisin, Ser. II, Vol. 29, 1976. (in Japanese with English abstract)
4. Housner, G. W., "Spectrum Intensities of Strong-Motion Earthquakes", Proc. of the Symposium on Earthquakes and Blast Effects on Structures, Earthquake Engineering Research Institute, 1952.
5. Kanai, K., "Earthquake Engineering", Kyoritsu Publishing. (in Japanese)

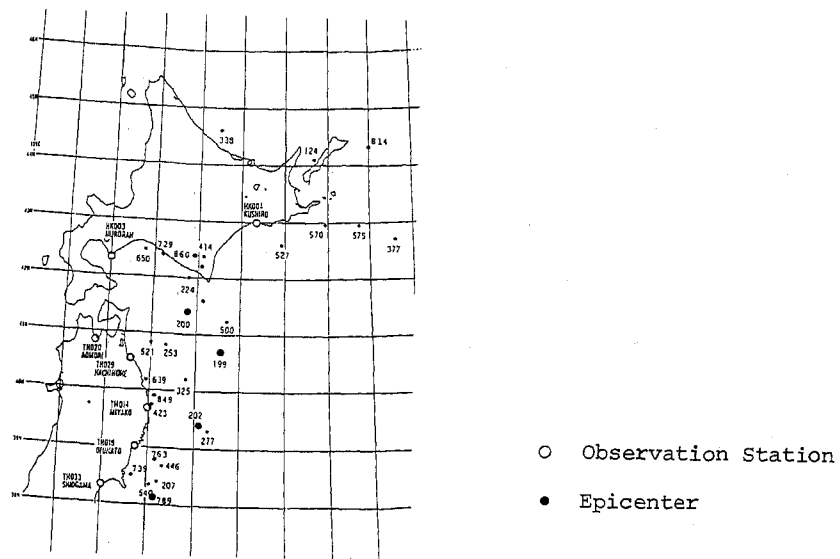


Fig. 1 Location of Observation Stations and Epicenters

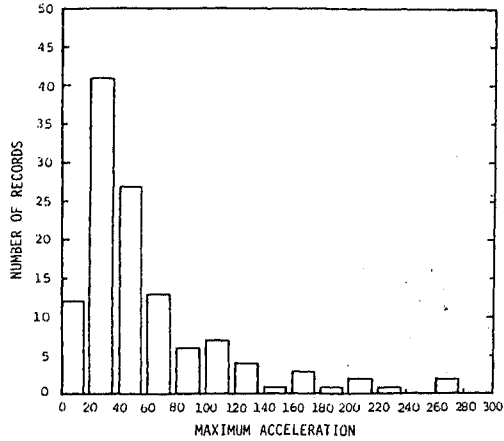


Fig. 2 Histogram for Maximum Accelerations of Strong Ground Motions, from 1965 to 1980

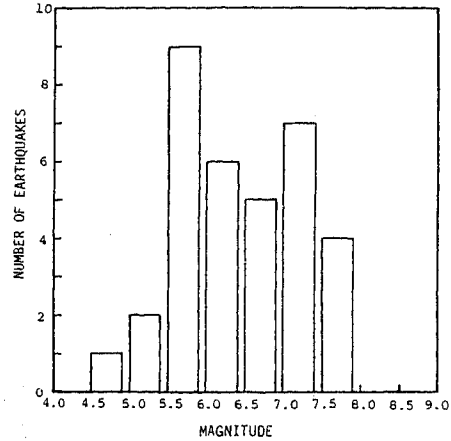


Fig. 3 Histogram for Magnitude

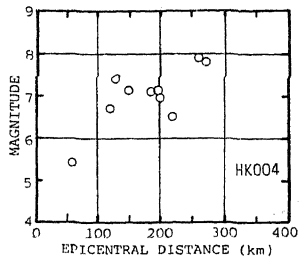


Fig. 4-a

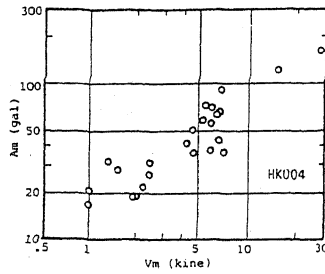


Fig. 5-a  
- Kushiro (HK004) -

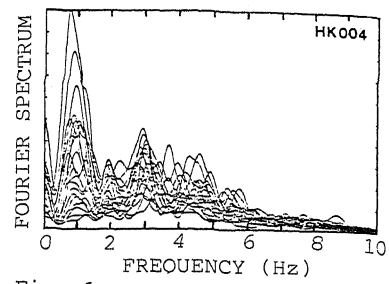


Fig. 6-a

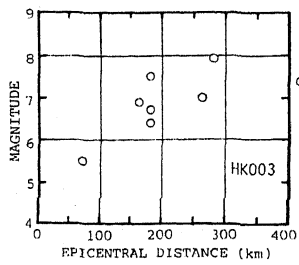


Fig. 4-b

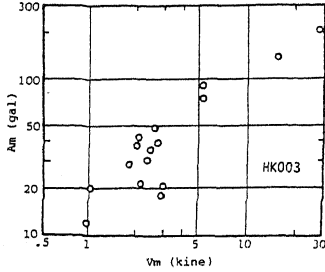


Fig. 5-b  
- Muroran (HK003) -

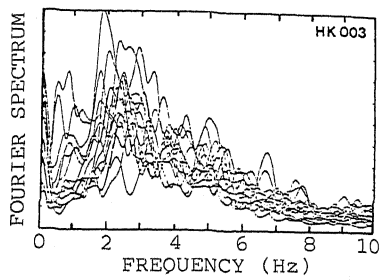


Fig. 6-b

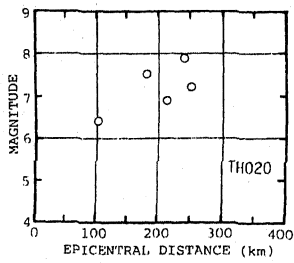


Fig. 4-c

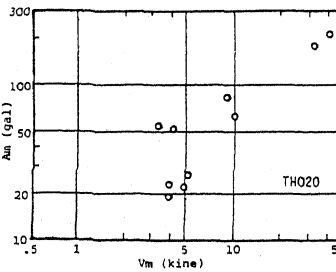


Fig. 5-c  
- Aomori (TH020) -

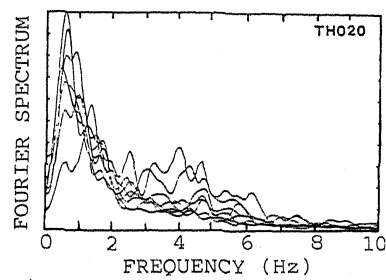


Fig. 6-c

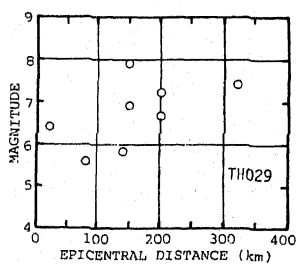


Fig. 4-d

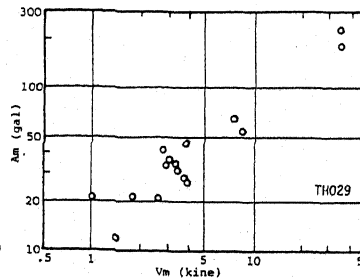


Fig. 5-d  
- Hachinohe (TH029) -

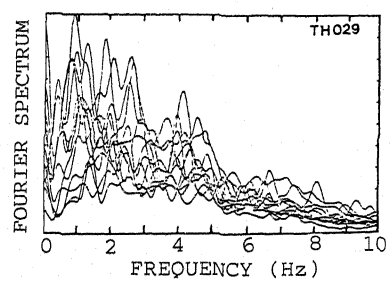


Fig. 6-d

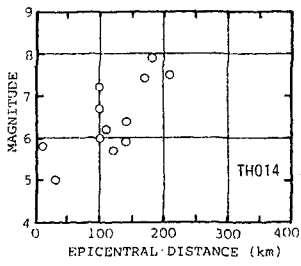


Fig. 4-e

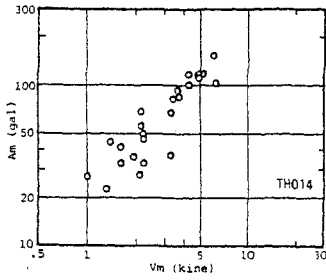


Fig. 5-e  
- Miyako (TH014) -

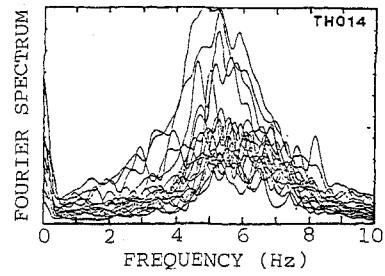


Fig. 6-e

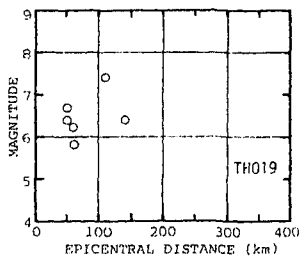


Fig. 4-f

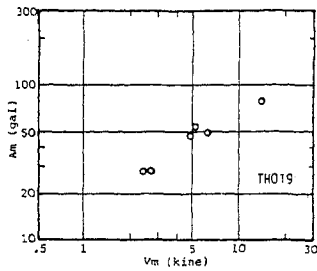


Fig. 5-f  
- Ofunato (TH019) -

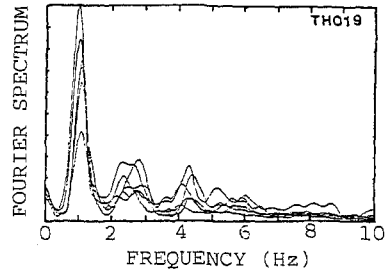


Fig. 6-f

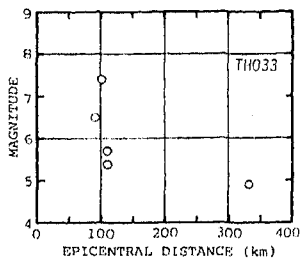


Fig. 4-g

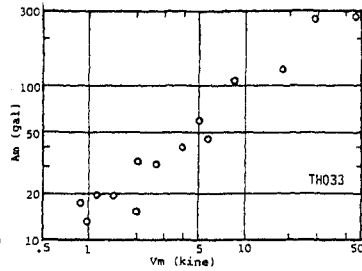


Fig. 5-g  
- Shiogama (TH033) -

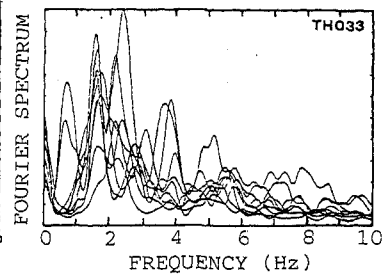
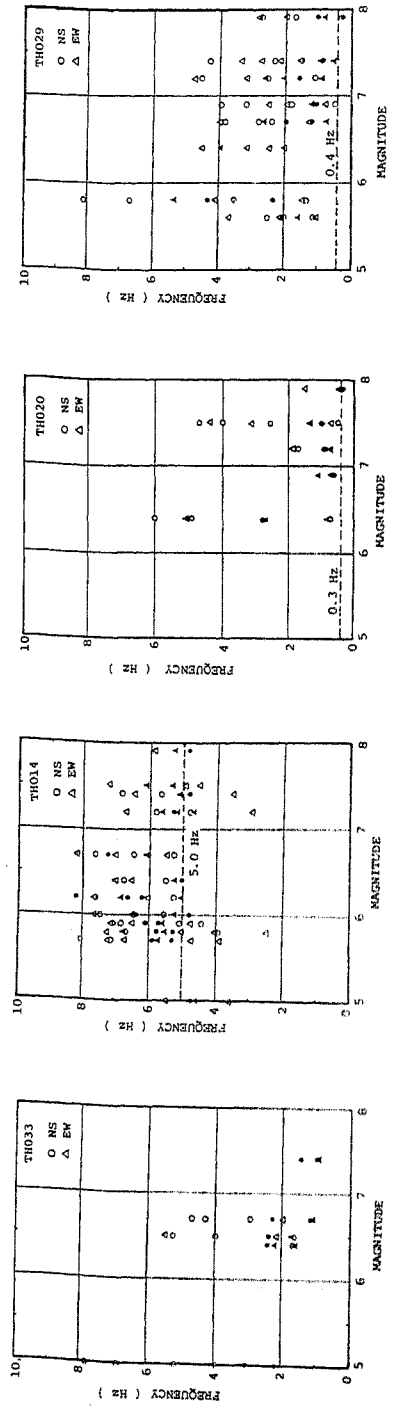


Fig. 6-g

Fig. 4 Scattergram for Magnitude versus Epicentral Distance

Fig. 5 Scattergram for Maximum Acceleration, Am, versus Maximum Velocity, Vm

Fig. 6 Fourier Spectrum of Strong Ground Accelerations (Band Width 0.4 Hz)



(a) Shiogama (b) Miyako (c) Aomori (d) Hachinohe

Fig. 7 Relationships between Magnitude and Predominant Frequencies

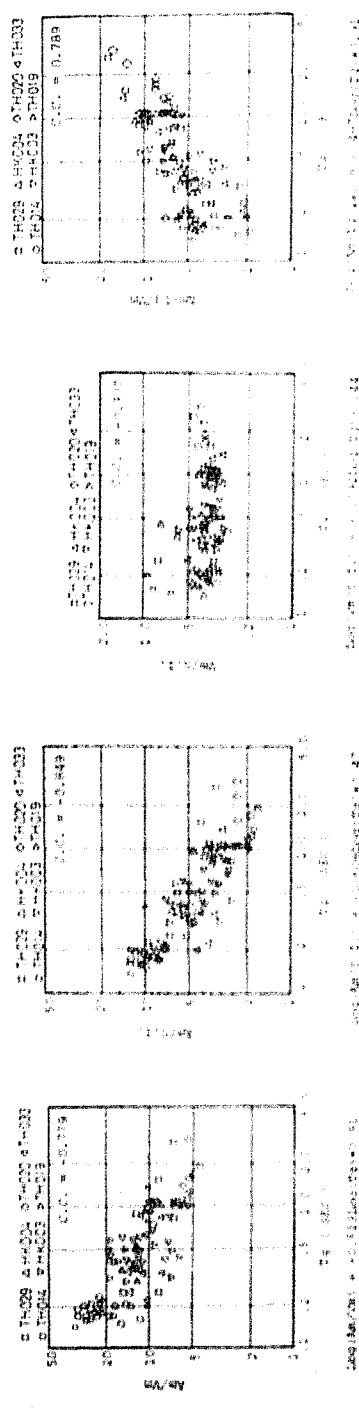


Fig. 8 Am/Vm versus Tg Fig. 9 Am/SI versus Tg Fig. 10 Vm/SI versus Tg Fig. 11 Am/Tg/Vm versus Tg

Am; Maximum Acceleration Vm; Maximum Velocity SI; Spectrum Intensity Tg; Predominant Period of Acceleration Records